

Lehigh University Lehigh Preserve

Fritz Laboratory Reports

Civil and Environmental Engineering

1975

The simplified subassemblage analysis of frames, May 1975

George C. Driscoll Jr.

Reinhard L. Gsellmeier

Follow this and additional works at: <http://preserve.lehigh.edu/engr-civil-environmental-fritz-lab-reports>

Recommended Citation

Driscoll, George C. Jr. and Gsellmeier, Reinhard L., "The simplified subassemblage analysis of frames, May 1975" (1975). *Fritz Laboratory Reports*. Paper 2018.
<http://preserve.lehigh.edu/engr-civil-environmental-fritz-lab-reports/2018>

This Technical Report is brought to you for free and open access by the Civil and Environmental Engineering at Lehigh Preserve. It has been accepted for inclusion in Fritz Laboratory Reports by an authorized administrator of Lehigh Preserve. For more information, please contact preserve@lehigh.edu.

Subassembly Analysis of Frames

THE SIMPLIFIED SUBASSEMBLY
ANALYSIS OF FRAMES

by

George C. Driscoll, Jr.
Reinhard L. Gsellmeier

FRITZ ENGINEERING
LABORATORY LIBRARY

This work has been carried out as part of an
investigation sponsored and funded jointly by
the following:

American Iron and Steel Institute
National Science Foundation
Joint Committee for the Planning and
Design of Tall Buildings

Fritz Engineering Laboratory
Department of Civil Engineering
Lehigh University
Bethlehem, Pennsylvania

May 1975

Fritz Engineering Laboratory Report No. 367.13

ACKNOWLEDGMENTS

This research was conducted at Fritz Engineering Laboratory, Lehigh University, Bethlehem, Pa., and was carried out as part of an investigation sponsored jointly by the American Iron and Steel Institute, National Science Foundation, and Joint Committee for the Planning and Design of Tall Buildings. Professor D. A. VanHorn is Chairman of the Civil Engineering Department and Professor L. S. Beedle is Director of Fritz Engineering Laboratory.

The authors wish to acknowledge the valuable contributions made by many other researchers in the development of the subassemblage method, and special thanks are extended to R. O. Disque of American Institute of Steel Construction who provided the ideas for some of the important simplifications used in this paper.

The authors also wish to extend their appreciation to Professor L. S. Beedle, who as Chairman of the Joint Committee for the Planning and Design of Tall Buildings provided his encouragement and assistance to the authors.

TABLE OF CONTENTS

ABSTRACT.	1
INTRODUCTION.	2
OBJECTIVE.	2
ASSEMBLAGE DESCRIPTION.	3
BASIC EQUATIONS.	4
SOLUTION PROCEDURE.	7
SOLUTION COMPARISON.	12
SUMMARY AND CONCLUSIONS.	13
FIGURES.	15
APPENDIX I - EXAMPLE LOAD VERSUS DRIFT CALCULATIONS.	25
APPENDIX II - REFERENCES.	39
APPENDIX III - NOTATION.	40

ABSTRACT

KEY WORDS: deflection; frames; plasticity; rigid frames; structural engineering; subassemblage

ABSTRACT: Simplifications and approximations to the original sway subassemblage method are developed which enable manual computation of the horizontal shear versus drift curve for a story in an unbraced multistory frame. A mathematical model called an assemblage is used to represent the story. Compatibility and equilibrium conditions for the story are investigated. A four step solution procedure is described: determination of initial and limiting states; girder moments and rotations to form a mechanism; subassemblage drift and shear resistance; and frame drift and shear resistance. An example set of calculations using this procedure is shown to compare favorably to a more exact computerized subassemblage solution.

THE SIMPLIFIED SUBASSEMBLAGE ANALYSIS OF FRAMES

INTRODUCTION

The sway subassemblage method of analysis was developed to assist in the evaluation of the horizontal shear versus drift characteristics of an individual story in an unbraced multistory frame (1, 2, 3, 4, 5, 6, 7). The purpose of this paper is to present some simplifications and approximations to the original sway subassemblage method which will enable the manual computation of shear versus story-drift in tabular form. The approach presented will avoid the necessity of graphical construction and tracing of restrained column curves which was required in the original presentation of the sway subassemblage method.

OBJECTIVE

The objective of the method is to find the relationship between horizontal drift Δ and horizontal shear ΣH on a single story of an unbraced multistory frame. A mathematical model called an assemblage will be used to represent the story. The assemblage will consist of the girders and a portion of the columns below the floor level extending down to a row of assumed inflection points. Furthermore the assemblage will be separated into subassemblages, each subassemblage consisting of one of the columns plus the girders framing into the column top.

The shear versus drift relationship for the assemblage will be determined by a displacement method during an assumed set of joint rotations θ . Changes in beam end moments during the rotations θ can be used to

determine other functions such as the column moments and the drift Δ . The relationship between these functions will be calculated as beam moments change from a state of at-rest equilibrium under factored vertical loads to a final state of combined vertical and lateral load equilibrium.

ASSEMBLAGE DESCRIPTION

Different boundary conditions are appropriate for assemblages modeling top, bottom and typical interior stories of a frame. The conditions for typical interior stories will be considered here.

A sketch of an assemblage for a three-bay frame is given in Fig. 1. The end thrust, shear, and moments of the columns above the floor are indicated by arrows but are not identified because their quantities do not enter the calculations which follow. For the assemblage sketched, the following assumptions will be made:

1. Each column will have an inflection point at a distance αh below the centerline of the floor girder. For typical multistory frames subjected to lateral loads, past solutions have shown that most columns have inflection points near midheight. This fact will be used here, as it has been used in the past, by assuming a value of α equal to 0.5 for typical interior stories.
2. The moment at the top of each column will be a portion β of the sum of the girder moments at the joint. For typical interior stories -0.5 will be assumed for β .

3. Moments and rotations will be assumed to be positive when acting in a clockwise direction on the end of a beam or column.

BASIC EQUATIONS

The total story shear ΣH must be in equilibrium with the total story column shears ΣQ . A portion of a typical column is sketched in Fig. 2 as a free body in the deflected position. The column shear Q (positive as shown in Fig. 2) may then be expressed in an equilibrium equation of the form

$$Q = -\frac{M_u}{\alpha h} - P \frac{\Delta}{h} \dots\dots\dots(1)$$

in which M_u = the end moment at the upper end of the column; P = the thrust in the column; h = the story height; α = the portion of story height from top of column to the inflection point; Δ = the story drift.

The angles in the free body of the column in Fig. 2 have the relationship

$$\frac{\Delta}{h} = \theta - \gamma \dots\dots\dots(2)$$

in which θ = the rotation of the joint; γ = the angle between the chord of the column segment and the tangent of the column centerline at the joint. It will be shown later that γ is a function of the column end moment.

Column end moments are determined from the equilibrium of moments around a joint as shown in Fig. 3. The sum of the girder moments to the right and left of the joint, called the restraining moment M_r , is defined as

$$M_r = M_{BL} + M_{BR} \dots\dots\dots(3)$$

in which M_{BL} = the end moment of the girder to the left of the joint;
 M_{BR} = the end moment of the girder to the right of the joint. The column
end moment at the upper end of the column below the joint may be found
from

$$M_u = \beta M_r \dots\dots\dots(4)$$

in which β = the portion of the restraining moment M_r resisted by column
end below the joint. For typical stories β is assumed equal to -0.5.

For the approximate method given in this paper, the column chord angle
 γ will be determined from

$$\gamma = \frac{M_u}{M_{pc}} \gamma' \dots\dots\dots(5)$$

in which M_{pc} = the reduced plastic moment of the column under its factored
axial load; γ' = the limiting column chord angle when the column end
moment is M_{pc} , and is computed as

$$\gamma' = \left[\left(22 - 20 \frac{P}{P_y} \right) \left(\frac{2\alpha h}{r_x} \right) - 20 \right] \times 10^{-5} \dots\dots\dots(6)$$

in which P = the thrust in the column; P_y = the plastic axial load and is
given by the product of the yield stress and area of the column; r_x = the
radius of gyration about the major principle axis of the column. The
function γ' was derived in Ref. 7 by fitting straight lines to the sway
subassemblage curves of Refs. 4 and 6. Its use permits direct computation
of approximate load versus sway behavior without referring to the curves.
Some errors on the unsafe side are introduced when the column moment ap-
proaches M_{pc} . It provides, however, a better approximation than the use

of $\gamma = (M_u \alpha h)/(3EI)$ which neglects all effects of column axial load.

Girder Restraining Characteristics. - Changes in girder moments which occur as the structure deforms are determined from relationships between the stiffness and the end rotation of adjacent girders. The far ends of the adjacent girders are subsequently restrained by the remaining members in the story. It is obviously not feasible to consider the influence of all members in a story. For practical design calculations it is sufficient to consider only the rotational restraining characteristics of the individual girder, as shown in Fig. 4. For simplification it is additionally assumed that both ends of a rigidly framed girder rotate through the same angle $\partial\theta$.

From elementary mechanics the change in girder end moment ∂M may be obtained as

$$\partial M = 6 \frac{EI}{L} \partial\theta \dots\dots\dots(7)$$

in which E = Young's modulus of elasticity; I = the strong axis moment of inertia of the girder; L = the length of the girder governing the bending stiffness (may be clear span; overall span will be conservative); $\partial\theta$ = the increment of end rotation of the girder. When a real or a plastic hinge is present at one end of a girder, the moment-rotation relationship becomes

$$\partial M = 3 \frac{EI}{L} \partial\theta \dots\dots\dots(8)$$

The terms $(6EI)/L$ and $(3EI)/L$ are the absolute stiffnesses of the girder. For many calculations, relative stiffnesses of I/L and $(0.5I)/L$ are sufficient to determine needed quantities with some saving in computation. This concept will be exploited in an example which will follow.

SOLUTION PROCEDURE

Solution of the load versus drift behavior of a story in a frame may be executed by a displacement method organized into the following four steps:

1. Determination of initial state and limiting state.
2. Girder moments and rotations to form a mechanism.
3. Subassemblage drift and shear resistance.
4. Frame drift and shear resistance.

Since the objective of the solution is to put together a piecewise linear load versus drift relationship it will be necessary to use certain variables in incremental form. This was done in Eqs. 7 and 8 by using increments $\partial\theta$ and ∂M . Equations 1 through 5 were presented in a static form for convenience. In the actual computation process, increments of certain variables such as ∂Q , ∂M , $\partial\Delta/h$, etc. will be used to distinguish their values from the cumulative values at the end of an increment.

The four steps in the solution will first be described in broad terms in order to outline the concepts. An example will follow which will illustrate in detail the computational procedure.

INITIAL STATE AND LIMITING STATE. - In the first step, structural parameters are tabulated as needed for the members selected in the trial story. The initial at-rest state of the story is then determined by a consideration of the story under factored vertical load alone (Fig. 5b).

Here an approximation of the beam end moments and column end moments is made by either a moment balance or a one-story moment distribution solution assuming no drift. Depending on the accuracy desired, equilibrium may be formulated based on center-to-center spans or on clear spans of the girders. If center-to-center spans are used, the fixed end moment FEM is computed as

$$FEM = 1.3 \frac{wL^2}{12} \dots\dots\dots (9)$$

in which 1.3 = the load factor for combined load; w = the distributed working load; L = the center-to-center span. If clear spans are used, the fixed end moments of the shorter span are transformed to beam moments at the column centerlines by the expression

$$FEM = 1.3 \frac{w}{12} (L - d_c) (L + 2d_c) \dots\dots\dots (10)$$

in which d_c = the average column depth flanking the girder clear span.

The other end of the behavior sequence is bounded by the limiting moments which are determined at the ends of each girder corresponding to its maximum capacity to resist wind while carrying the appropriate factored transverse loads (Fig. 5e). The limiting moments may be determined from design aids prepared for preliminary design. In fact, the limiting moments will usually have been determined during the preliminary design.

GIRDER MOMENTS AND ROTATIONS. - The second step of the solution procedure consists of determining the sequence of formation of plastic hinges in the girders of a subassemblage. During a set of joint rotation increments θ the girder end moments are caused to change from the initial

at-rest state under vertical load to the final combined load state. For each girder in a subassemblage the initial girder end moment is subtracted from its corresponding final moment value to find the possible total change in moment. Each of these possible total changes in moment is divided by the corresponding stiffnesses of Eqs. 7 or 8 to find the amount of rotation necessary to reach the limiting state. The least rotation of all those computed is selected as the controlling increment; it will usually occur at the lee end of a girder. The change in moment at each end of each girder in the subassemblage due to the same rotation is then determined from the stiffness equations. Figs. 5c and 5d show the form of increments to the moment diagram. The changes in end moments are added to the prior state to determine the new intermediate moments. Eqs. 3 and 4 may then be used to determine the column end moment below a joint in order to check for a column plastic hinge. After a plastic hinge forms at one end of a girder, the stiffness is reduced to zero at that end and to half the original value at the far end. The process is then repeated by finding a new set of possible changes in end moments and joint rotations. For an interior subassemblage with all moment-resisting connections, up to four plastic hinges may be required to form a mechanism. For a lee exterior subassemblage only one plastic hinge is required and for a windward exterior subassemblage up to two plastic hinges may be required. For either an interior or exterior subassemblage, however, the formation of a plastic hinge in the column will form a mechanism. When the plastic hinge sequence has been determined within each subassemblage in a story, the rotations and corresponding column moment values are saved for use in the next step of the solution.

SUBASSEMBLAGE DRIFT AND SHEAR RESISTANCE. - In the third step of the sway subassembly solution, the column moment increments ∂M_u and the joint rotation increments $\partial \theta$ obtained from the second step are used to determine the drift and shear resistance of the subassembly. Fig. 6 shows a typical plot of shear versus drift for a subassembly.

For each increment, the value of the column chord angle $\partial \gamma$ can be determined from ∂M_u by using Eqs. 5 and 6. The subassembly sway increment $\partial \Delta/h$ may then be determined from Eq. 2. Finally the increment of shear ∂Q may be obtained from Eq. 1 by using the values already determined for ∂M_u and $\partial \Delta/h$ along with the tabulated value of P . The cumulative values of Q and Δ/h at the end of each increment may be obtained by adding the incremental values ∂Q and $\partial \Delta/h$ to the previous cumulative values as

$$Q_{\text{new}} = Q_{\text{old}} + \partial Q \dots\dots\dots(11)$$

$$\left(\frac{\Delta}{h}\right)_{\text{new}} = \left(\frac{\Delta}{h}\right)_{\text{old}} + \frac{\partial \Delta}{h} \dots\dots\dots(12)$$

For use in the last stage of the subassembly calculation, slope values $\partial Q/(\partial \Delta/h)$ are recorded for each subassembly for each increment. Other data to be used in the next step are the initial shear Q in each subassembly, $\partial \Delta/h$ values at the end of each increment, and the overall sequence of Δ/h values for formation of each plastic hinge in the story.

One further concept is of interest in the subassembly. After formation of a mechanism, the change in restraining moment ∂M_u at the top of the column will be zero since either the restraining members or the column lose their stiffness. Then the incremental form of Eq. 1 reduces

to the expression

$$\partial Q = -P \left(\frac{\partial \Delta}{h} \right) \dots\dots\dots(13)$$

The slope of the Q versus Δ/h curve is thus $-P$ which means that as the drift increases the shear on the column must be reduced to maintain equilibrium. In a single subassembly this means disaster because the overturning moment of the vertical loads will cause collapse. In a trial story, however, the other columns will assume greater shares of the horizontal shear enabling the subassembly with an early-forming mechanism to "take a free ride". Through this process the total story can accept increasing horizontal force after some subassemblies have formed mechanisms.

FRAME DRIFT AND SHEAR RESISTANCE. - Once the subassembly drift and shear resistance have been determined, all necessary data are available to determine the drift and shear resistance of the total story. The fourth step of the sway subassembly procedure is simply the addition of the Q values of all columns in the story at common values of Δ/h . This is shown schematically in Fig. 7. For a single subassembly the relationship can be expressed as

$$Q_{\text{new}} = Q_{\text{old}} + \left(\frac{\partial Q}{\partial \Delta} \right) \left[\left(\frac{\Delta}{h} \right)_{\text{new}} - \left(\frac{\Delta}{h} \right)_{\text{old}} \right] \dots\dots\dots(14)$$

This equation may be used so long as no new plastic hinge forms between the old and new values of Δ/h . At the time a new plastic hinge forms, the value of the slope $\partial Q / (\partial \Delta/h)$ must be changed for the subassembly affected. The use of Eq. 14 to add an increment to the shear versus drift curve is depicted in Fig. 8.

For a complete story, Eq. 14 may be used with the substitution of ΣQ_{old} as the summation of shears for all columns and $\Sigma[\partial Q/(\partial \Delta/h)]$ as the summation of graph slopes for all subassemblages. This results in an expression for ΣQ_{new} , the summation of cumulative shears for all columns, in the form

$$\Sigma Q_{new} = \Sigma Q_{old} + \Sigma \left[\frac{\partial Q}{\left(\frac{\partial \Delta}{h} \right)} \right] \left[\left(\frac{\Delta}{h} \right)_{new} - \left(\frac{\Delta}{h} \right)_{old} \right] \dots (15)$$

After all plastic hinges have formed, the total slope of the Q versus Δ/h curve is $-\Sigma P$. In calculations made in the example, the curves have been projected to a Δ/h value of 0.025 radians to show the shape of the unloading function. Typically, the maximum shears are reached at Δ/h values of between 0.005 and 0.010.

SOLUTION COMPARISON

In Appendix I an example is given showing the load versus drift calculations for a story 14 levels from the top of a 24 story unbraced frame using the simplified subassemblage analysis procedure presented in this paper. Fig. 9 compares the load versus drift curve for this story as calculated by this example to a load versus drift curve based on calculations made using a computerized version of the subassemblage analysis procedure described in Ref. 5. The simplified subassemblage analysis gives both a slightly higher elastic stiffness and ultimate strength than the computerized subassemblage analysis. This is explained by the assumption made in the simplified method that the members to which a girder is connected (the columns and adjacent girders) are perfectly rigid. Thus the corresponding

joint rotational restraint of the end of a girder is given as $(6EI)/L$. On the other hand, the computerized analysis considers the flexibility of the members to which the girder is connected, with the result that the corresponding joint rotational restraint at the end of a girder is slightly less than $(6EI)/L$. The resultant difference between the two load versus drift curves is very small, however, and for practical design considerations this difference can be ignored.

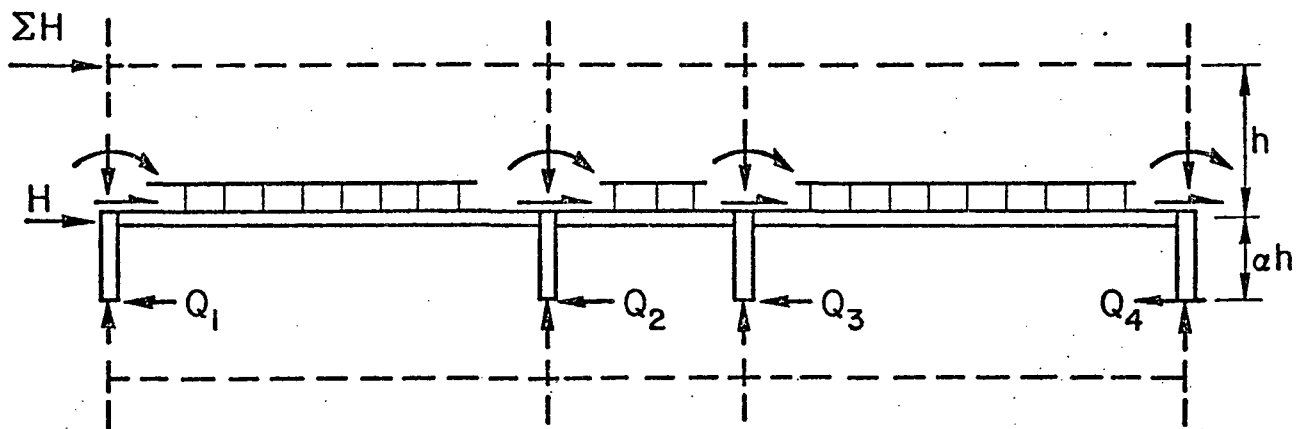
SUMMARY AND CONCLUSIONS

In the early days of tall building construction when steel frameworks were designed using high factors of safety and were usually shrouded in a very heavy masonry or stone cladding, deflection problems were justifiably considered to be of secondary importance. In the modern era of plastic design, however, with the inherent lighter, more flexible frames coupled with lighter exterior cladding, deflections have become much more critical and in some instances even govern the design of a building. Unfortunately, the process of calculating deflections has always been a rather arduous task for engineers, particularly beyond the elastic range. The subassemblage method of analysis was thus developed to greatly simplify and reduce the calculations required to arrive at the lateral load versus sway relationship for a story in a frame.

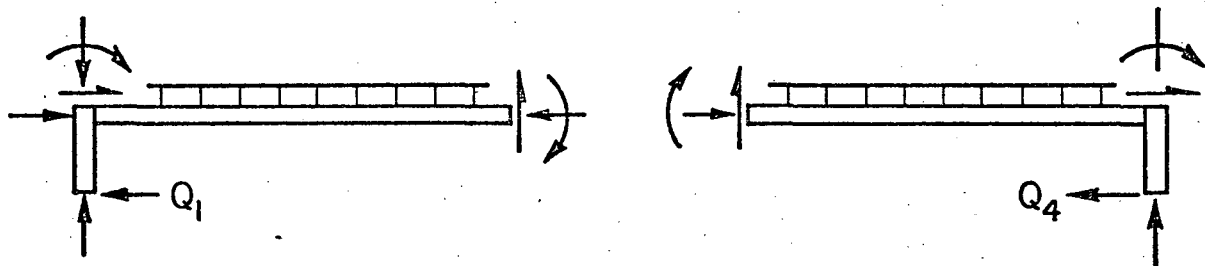
In this paper a simplified subassemblage analysis procedure was presented to allow deflection calculations to be made by hand without the aid of a computer or the necessity of graphical construction and tracing of restrained column curves. This method has been shown to be sufficiently accurate to an exact subassemblage analysis for practical design office

applications. It should be pointed out, however, that the subassemblage method does not consider the additional sway induced by chord drift. In the middle and lower stories of a frame chord drift is small enough to be neglected without inducing appreciable error. In the upper stories of a frame where chord drift is prominent, an overestimation of the load versus sway stiffness in the elastic range is given by a subassemblage analysis, but the predicted ultimate strength of the story is affected only very slightly.

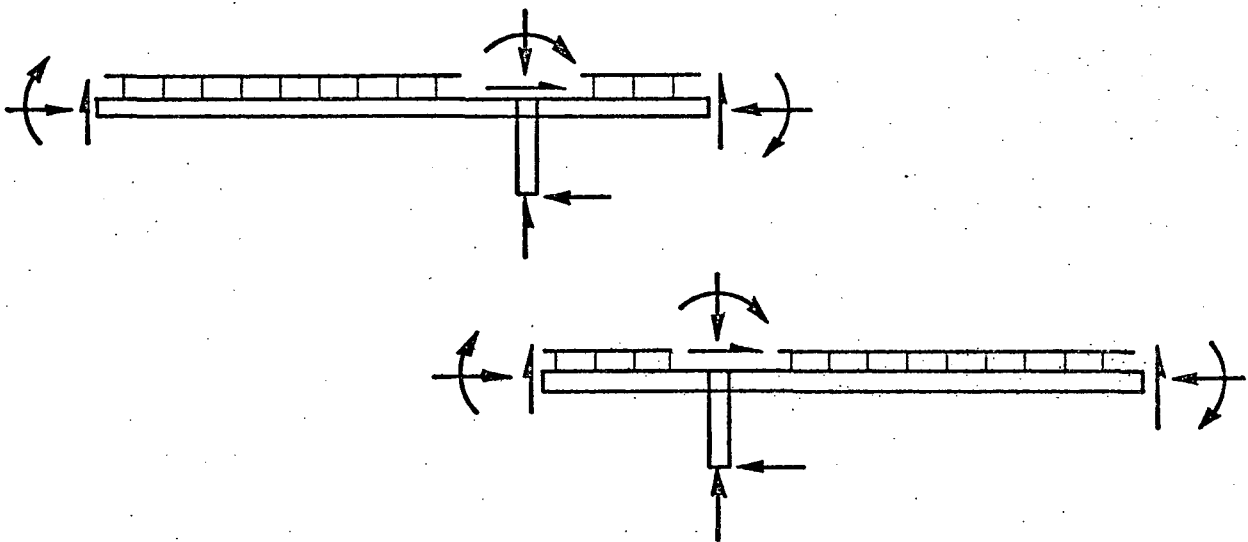
FIGURES



(a) One - Story Assemblage

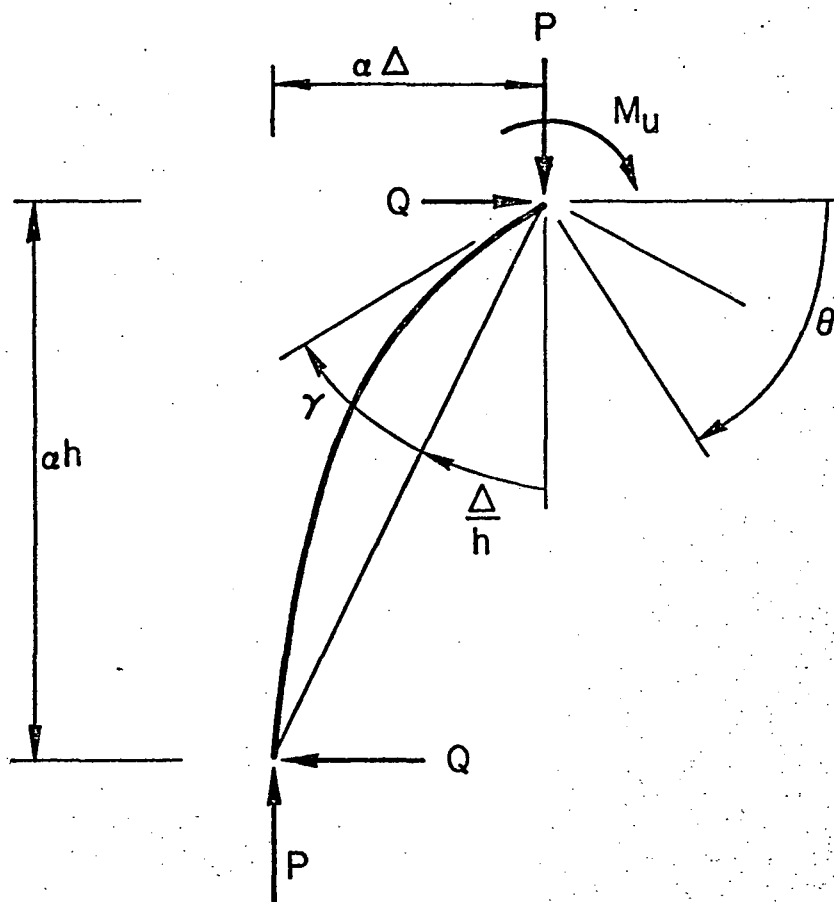


(b) Exterior Subassemblages



(c) Interior Subassemblages

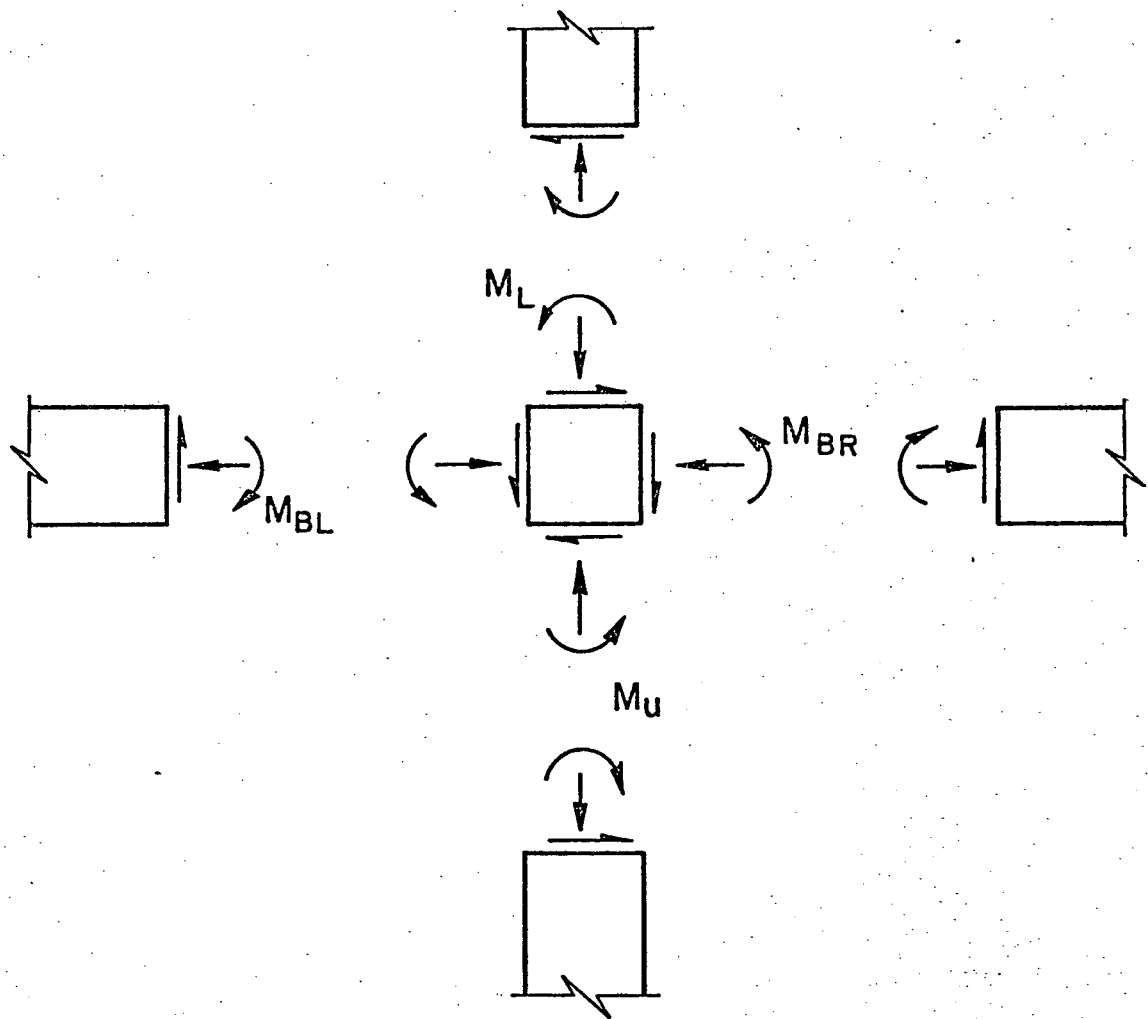
Fig. 1 ASSEMBLAGE AND SUBASSEMBLAGES



$$Q = \frac{-M_u}{\alpha h} - \frac{P\Delta}{h}$$

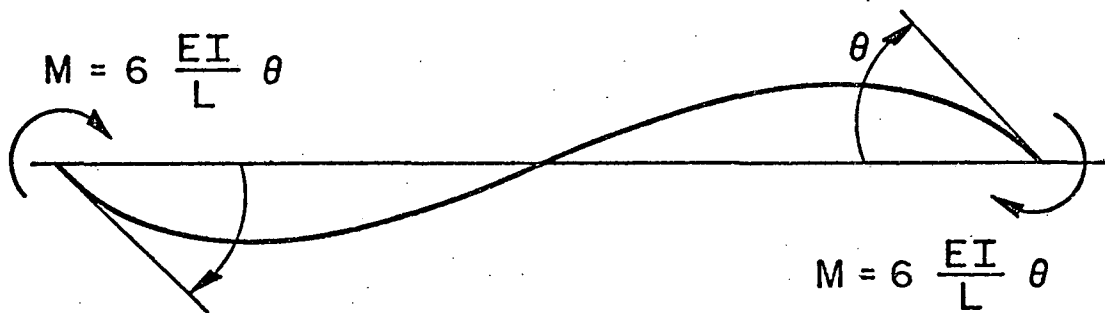
$$\frac{\Delta}{h} = \theta - \gamma$$

Fig. 2 FREE BODY SKETCH OF PORTION OF COLUMN

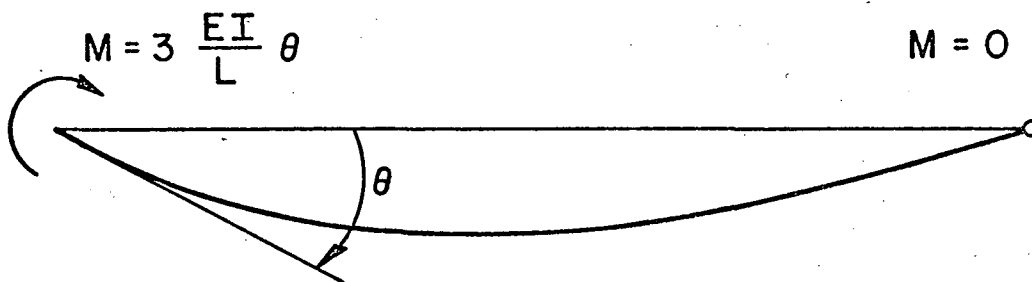


$$M_u = \beta (M_{BL} + M_{BR})$$

Fig. 3 FREE BODY SKETCH OF JOINT

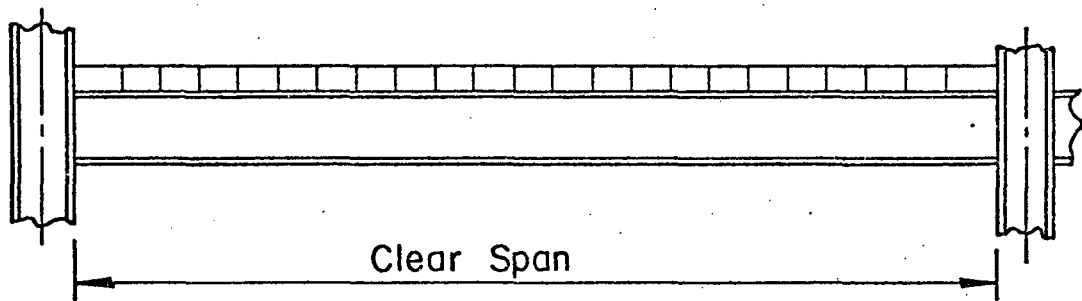


(a) Two Ends Rigid

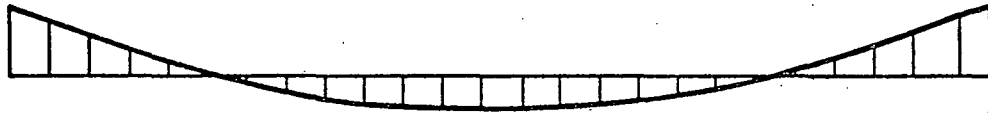


(b) One End Hinged

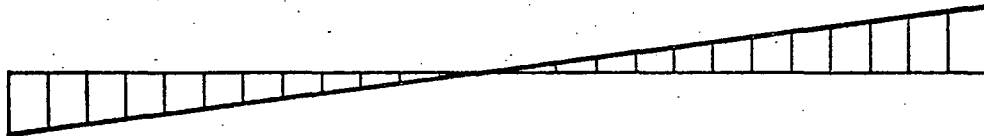
Fig. 4 BEAM MOMENT CHANGES CAUSED BY END ROTATION



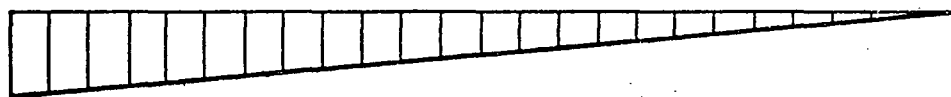
(a) Rigidly Framed Beam



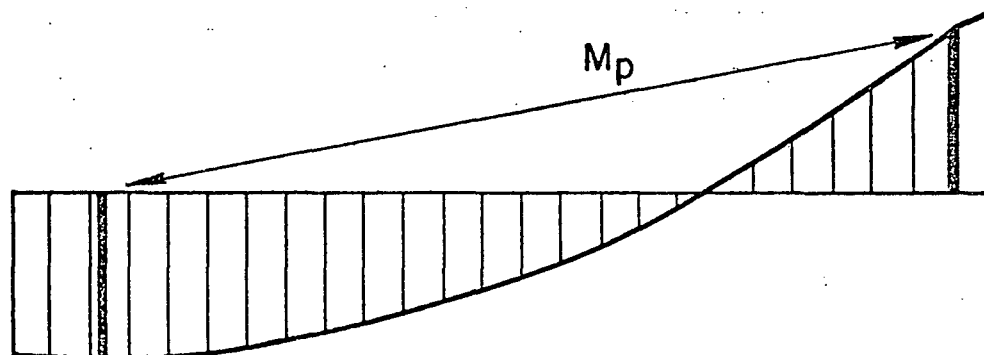
(b) Initial Moments



(c) Moment Changes With Elastic Ends



(d) Moment Changes With Plastic Hinge or Real Hinge at Right End



(e) Final Moments

Fig. 5 WIND MOMENT EFFECTS ON A BEAM

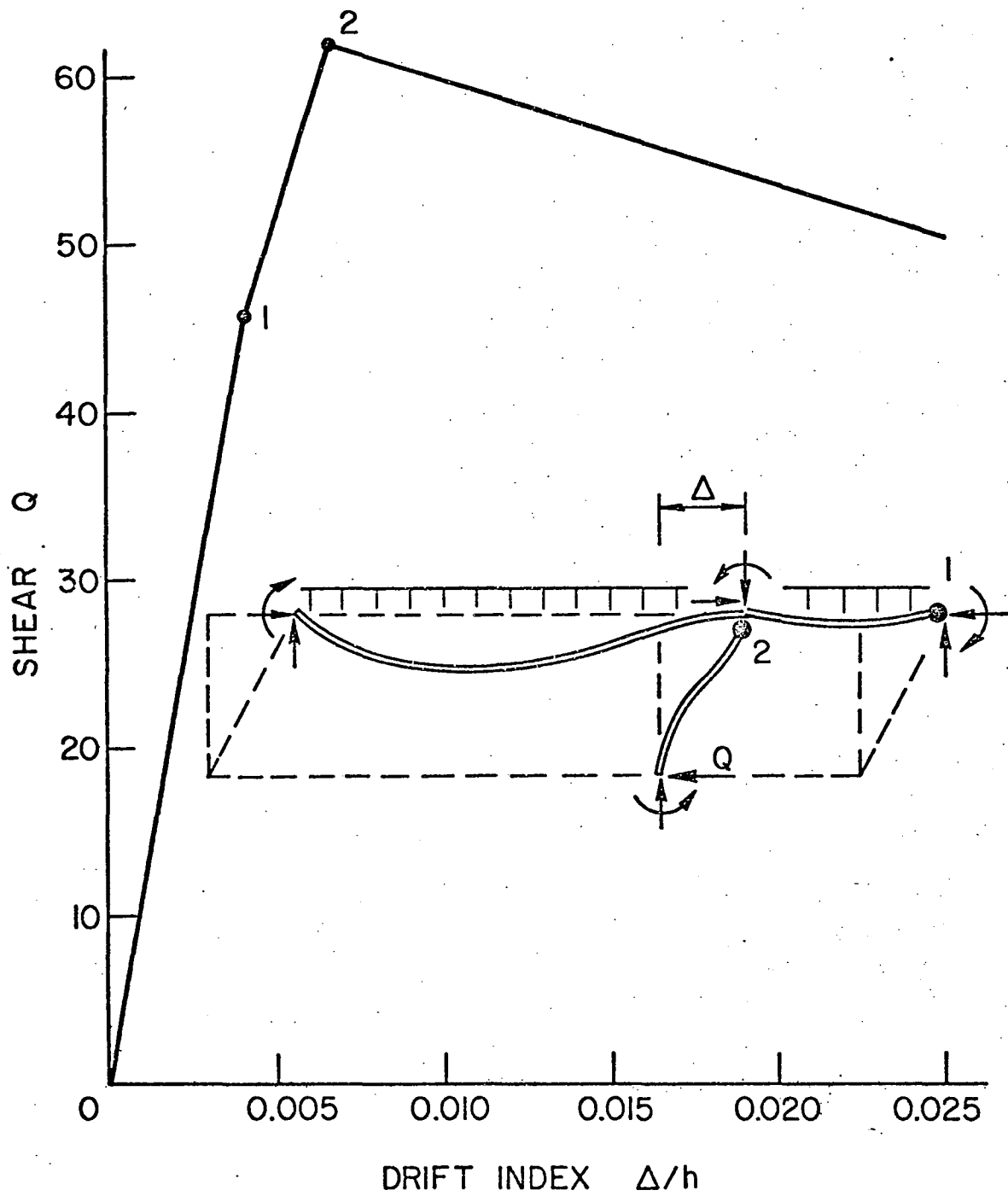
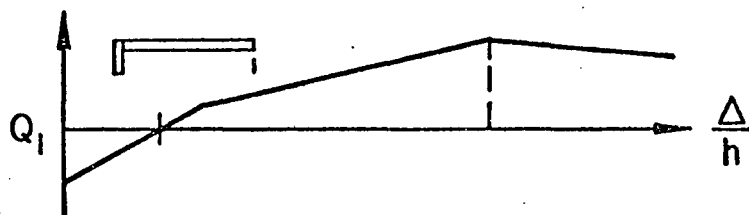
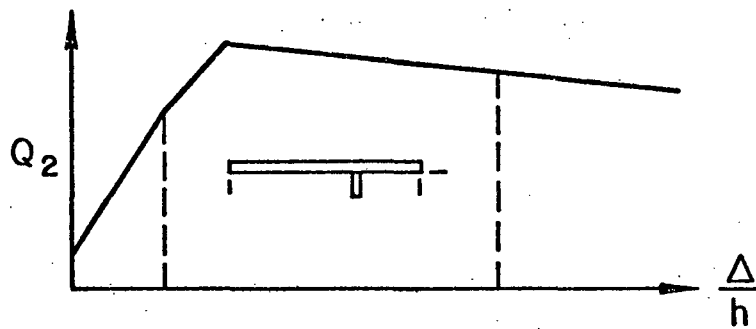


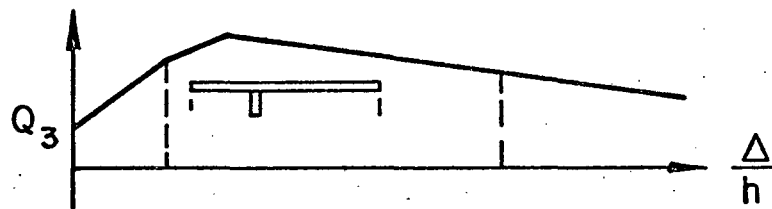
Fig. 6 SUBASSEMBLY DRIFT AND SHEAR RESISTANCE



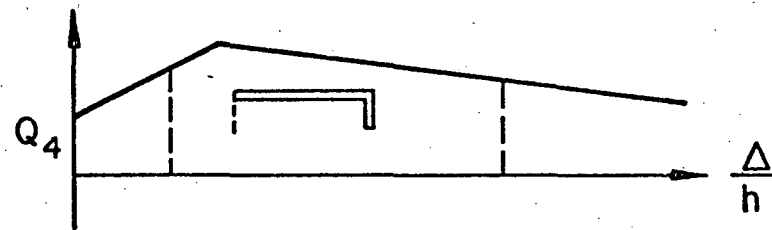
(a)
Subassemblage 1



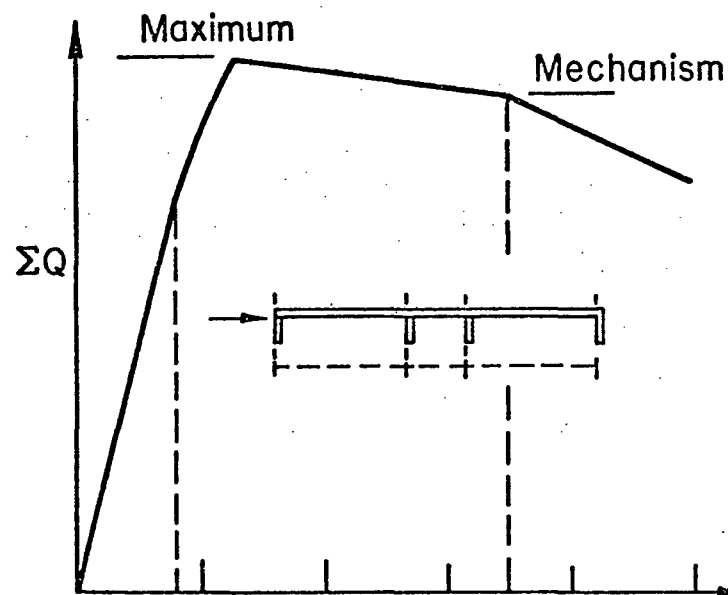
(b)
Subassemblage 2



(c)
Subassemblage 3



(d)
Subassemblage 4



(e)
One - Story
Assemblage
Lateral Load
vs
Drift

Fig. 7 LOAD vs. DRIFT CURVES

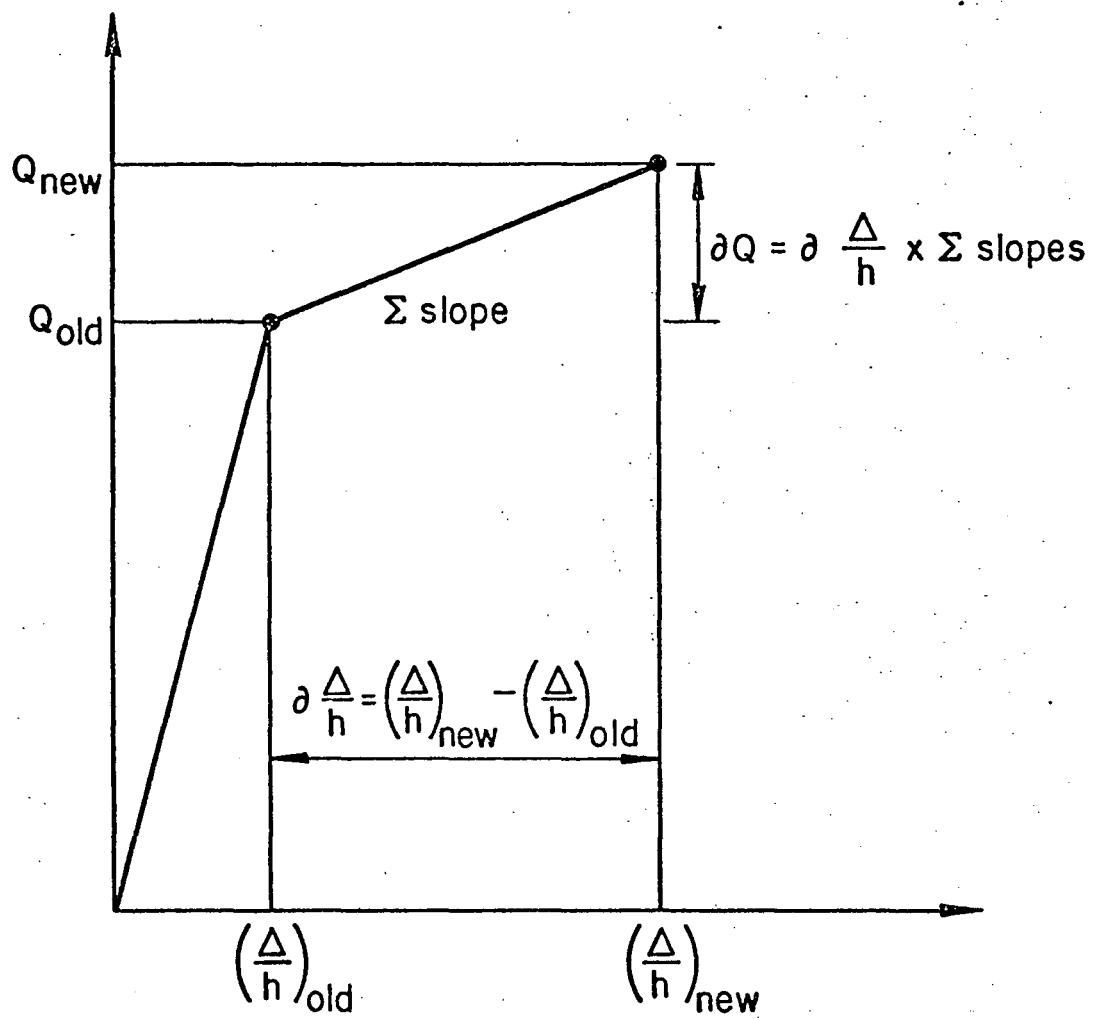


Fig. 8 CONCEPT OF SUMMATION PROCEDURE FOR Q

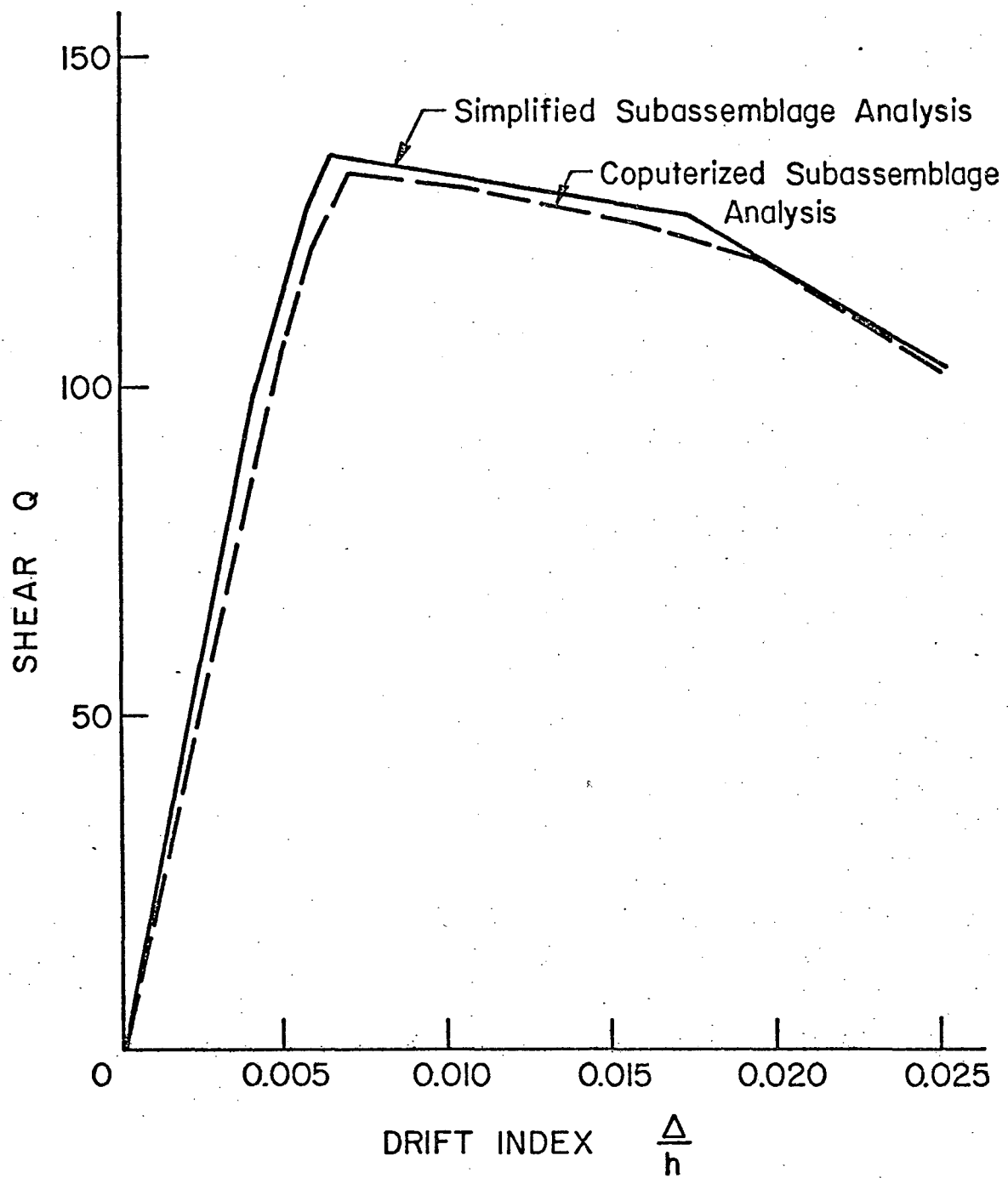


Fig. 9 COMPARISON OF STORY SHEAR vs. DRIFT ANALYSIS

APPENDIX I. - EXAMPLE LOAD VERSUS DRIFT CALCULATIONS

This appendix illustrates the calculations required to construct the load versus drift curve for the story shown in Fig. A1. The given story has all rigid connections, and the column axial loads are based on a preliminary design of the entire frame. The distributed girder loads have all been factored by 1.3, and the wind is assumed to come from the left (due to symmetry, the response for wind from the right is identical). Calculations are given in tables which are meant to be self-explanatory, therefore only brief comments will be made about them here.

TABLE A1:

- (1) Lines 1-8. - Properties of columns are listed and calculated.
- (2) Lines 9-10. - Initial moments and shears calculated in Table A2 are listed.
- (3) Lines 11-15. - Values are calculated for γ' using Eq. 6.
- (4) Lines 16-24. - Girder properties are listed and relative stiffnesses are calculated.

TABLE A2: Fixed end moments based on Eq. 10 are calculated and used in a moment distribution procedure to obtain at-rest gravity moments. Modified stiffnesses recognizing symmetry and hinges make it possible to isolate the assemblage from the rest of the structure in obtaining an estimate of initial beam and column end moments and shears.

TABLE A3: Limiting moments at each end of each girder are calculated for use in further steps.

- (1) Lines 1-5. - Initial data are tabulated.
- (2) Lines 6-16. - Dimensionless parameters are calculated.

(3) Lines 17-18. - Dimensionless values of end moments are calculated for girders with both ends rigid.

(4) Lines 19-22. - Alternate computational procedures are provided for beams with real hinges.

(5) Lines 23-24. - Dimensional values of end moments are calculated and recorded, including values of wind in either direction for unsymmetrical structures.

TABLES A4 and A5: Changes in moments and relative rotation of joints during formation of each plastic hinge are calculated based on either Eqs. 7 or 8. A column of calculations is required for each end of each girder in the subassemblage. Thus subassemblage A requires columns for both ends of girder AB while subassemblage B requires two columns each for girders AB and BC. Similarly the calculations for subassemblage C and D are given in Table A5.

(1) Lines 1-3. - Limiting moments are entered from Table A3 and initial moments from Table A2.

(2) Line 4. - For convenience of computation a relative stiffness coefficient of 1, 1/2, or 0 is assigned for girders, depending on whether both the near and far ends of a girder are fixed or free to rotate. This implies that a term of $6E$ is omitted from each stiffness coefficient along with a factor to adjust for length dimensions.

(3) Line 5. - The relative stiffness coefficient is multiplied by the girder moment of inertia and divided by the clear span. To adjust for clear span statics, the relative stiffness may be multiplied by $(1 - d_c/L)$ as given on line 24 of Table A1.

(4) Line 6. - The sum of the girder stiffnesses on each side of the column is entered.

(5) Line 7. - This implies solution of either Eqs. 7 or 8 for the relative rotation increment.

(6) Line 8. - For each sumassemblage, the least increment of joint rotation to form a plastic hinge in that subassemblage is recorded. Each subassemblage is treated separately, even when the same girder is shared by two adjacent subassemblages.

(7) Lines 9-10. - Moment increments corresponding to the selected rotation increments are calculated and added to initial moments to find the current state of end moments for girders and columns.

(8) Lines 11-12. - The column moment is checked for a possible plastic hinge. The value of the column moment is determined from the sum of the girder end moments as described by Eq. 4.

(9) Line 13. - The hinge formed is identified for each subassemblage so that proper changes can be made to the relative stiffness coefficients.

(10) Line 15. - New relative stiffness coefficients reflect the formation of the previous plastic hinge in each subassemblage.

(11) Lines 16-24. - These steps repeat the operations of Lines 5 to 13 using the revised stiffnesses.

In most typical cases subassemblages B and C would require the formation of three or four plastic hinges before a mechanism developed. In this example, formation of a plastic hinge in each column produced a mechanism.

Certain extra steps in Tables A4 and A5 are inserted between lines to assist in checking for column plastic hinges. In Table A4 for instance, a total value of limiting girder moments based on a plastic hinge in column B is listed. The value of 635.8 is determined from Eq. 4 by setting M_u equal to the M_{pc} value of -317.9 and β equal to -0.5. Above line 14, the new total ΔM possible is 635.8 minus the girder end moment sum at the joint. Above line 18, the relative rotation of the joint to form a column

plastic hinge is $171.8/72.35$ to give a value of 2.38 which is less than the value required to cause a plastic hinge in either of the girders.

TABLE A6: In this table the increments of shear ∂Q and the corresponding increments of drift $\partial \Delta/h$ are determined from Eqs. 1, 2 and 5. Although the calculations for each subassembly are listed side-by-side, they are independent of each other.

(1) Line 1. - The relative rotation is entered from either Lines 8 or 19 of Tables A4 and A5.

(2) Line 2. - The change in column moment ∂M_u is calculated from either Lines 1 or 17 of Tables A4 and A5.

(3) Line 3. - Eq. 5 is used to calculate γ , using the value of γ' given in Line 15 of Table A1.

(4) Line 4. - The relative rotation $\partial \theta$ is converted to radians by multiplying by $144/(6E)$.

(5) Line 5. - The increment of drift $\partial \Delta/h$ is calculated by Eq. 2.

(6) Lines 6-8. - The increment of shear ∂Q is calculated by Eq. 1.

(7) Lines 9-12. - Initial data is obtained from Table A2, increments are added, and the results are identified as DATA 1 and DATA 2.

(8) Line 13. - The total sequence of Δ/h values to be used in summing the effect for the complete story is determined after all other calculations in this table have been completed.

(9) Line 14. - The slope for the given increment of the subassembly Q versus Δ/h curve is calculated for later use in the summation process.

(10) Lines 15-26 and 27-38. - Lines 1 to 14 are repeated for another cycle.

After a mechanism has formed in a subassembly, the increment of drift is arbitrary and the shear is $-P\Delta/h$. The last increment of drift is selected to bring the total drift to 0.025 radians.

TABLE A7: The Q versus Δ/h relationship is calculated for the story by Eq. 13. One column of the computation form is provided for each sub-assembly plus one for the total story and one for identifying the Δ/h sequence given in Lines 13, 25 and 37 of Table A6. It is seen that only the line giving the graph slope for each subassembly must be completely filled out for each sequence. If desired, all columns may be filled in for each line, thus giving the shear versus drift curve for each subassembly separately as a cross check.

(1) Lines 1-4. - Data is entered from Table A6. The slopes in Line 3 are summed algebraically to give the total slope for the story.

(2) Line 8. - The subassembly which forms a hinge at the end of each Δ/h sequence (see Table A6, DATA 4) is identified as a reminder to change the slope in that column.

(3) Lines 9, 15, 21, 27, 33, 39 and 45. - The new graph slope is inserted for the affected subassembly and all the slopes are summed.

(4) Lines 10-14, 16-20, 22-26, 28-32, 34-38, 40-44 and 46-50. - The sequence of Lines 4 to 8 is repeated.

Upon completion of the calculations, the results may be plotted for each set of Q and Δ/h values, as in Fig. 9.

TABLE A1. - COLUMN AND GIRDER PROPERTIES

Line	Function	Operation	Units	Column			
				A	B	C	D
①	Size			W14x111	W14x111	W14x111	W14x111
②	P		kips	626	626	858	812
③	P _y		kips	1180	1180	1180	1180
④	P/P _y	② / ③		0.531	0.531	0.726	0.688
⑤	h		feet	9.66	9.66	9.66	9.66
⑥	r _x		inches	6.23	6.23	6.23	6.23
⑦	h/r _x	$\frac{12.0 \times ⑤}{⑥}$		18.65	18.65	18.65	18.65
⑧	M _{pc}		kip-feet	317.9	317.9	188.6	214.2
⑨	M _c ^o	Table A2	kip-feet	68.8	-43.0	43.0	-68.8
⑩	Q _o	$(-2.0 \times ⑨) / ⑤$	kips	-14.23	8.90	-8.90	14.23
⑪	20P/P _y	20.0 x ④	radians	10.62	10.62	14.52	13.76
⑫	22.0 - 11	22.0 - ⑪	radians	11.38	11.38	7.48	8.24
⑬	$\frac{h}{r_x} (22 - 20 \frac{P}{P_y})$	⑦ x ⑫	radians	212	212	139.5	153.8
⑭	γ' x 10 ⁻⁵	⑬ - 20.0	radians	192	192	119.5	133.8
⑮	γ'	10 ⁻⁵ x ⑭	radians	0.00192	0.00192	0.00120	0.00134
				Girder			
				AB	BC	CD	
⑯	Size			W18x55	W18x45	W18x55	
⑰	I		inches ⁴	891	706	891	
⑱	L		feet	27	12	27	
⑲	M _p		kip-feet	336	269	336	
⑳	I/L	⑰ / ⑱	$\frac{\text{inches}^4}{\text{feet}}$	33.0	58.9	33.0	
㉑	L _g		feet	25.80	10.80	25.80	
㉒	I/L _g	⑰ / ㉑	$\frac{\text{inches}^4}{\text{feet}}$	34.5	65.4	34.5	
㉓	d _c /L		radians	0.0444	0.10	0.0444	
㉔	$\frac{I}{L_g} \times (\frac{1}{1 - d_c/L})$		$\frac{\text{inches}^4}{\text{feet}}$	36.1	72.5	36.1	

TABLE A2. - INITIAL MOMENTS AND SHEARS
USING MOMENT DISTRIBUTION^a

FEM = $\frac{1}{12} w (L-d_c) (L+2d_c)^b$ $d_c = 1.20$						
L	L-d _c	L+2d _c	w	$\frac{w}{12} (L-d_c) (L+2d_c)$	Girder	Column: $\frac{3}{4} \frac{I}{h}$
27	25.80	29.40	2.31	146.0	36.1	197.0
12	10.80	14.40	3.84	51.0	72.5	



ΣK_1 (relative)	DF ₁	ΣK_2 (relative)	DF ₂
36.1	0.0840	36.1	0.0775
197.0	0.458	36.25	0.0780
197.0	0.458	197.0	0.422
		197.0	0.422
$\Sigma = 430.1$	$\Sigma = 1.000$	$\Sigma = 466.35$	$\Sigma = 1.000$

Moment Balance

Joint	\updownarrow	\rightarrow	\leftarrow	\updownarrow	\rightarrow
DF	0.916	0.0840	0.0775	0.844	0.0780
FEM		-146.0	146.0		-51.0
	133.7	12.3	6.2		
		-3.9	-7.8	-85.5	-7.9
	3.6	0.3			
Final M	137.3	-137.3	144.4	-85.5	-58.9
Each column = $\frac{1}{2}$	68.6			-42.8	
$Q_o = -\frac{M_u}{4.83}$	-14.23			8.90	

^aSymmetry and hinges allow modified stiffnesses to be used.

^bFixed end moments are based on clear spans.

TABLE A3. - LIMITING MOMENTS

Line	Function	Operation	Units	Girder AB	Girder BC	Girder CD
①	M_{pm}	Trial Design	kip-feet	96.1	28.7	96.1
②	Section	Trial Design		W18x55	W18x45	W18x55
③	Z	Trial Design	inches ³	112	89.7	112
④	M_p	Trial Design	kip-feet	336	269	336
⑤	d_c/L		radians	0.0444	0.10	0.0444
⑥	$R = M_p/M_{pm}$	④ / ①		3.49	9.38	3.49
⑦	$G = 2.0 \times \text{⑥}$	(when ⑥ ≥ 4.0) ^a			18.76	
⑧	$G = 8.0(\text{⑥}^{1/2} - 1.0)$	(when ⑥ < 4.0) ^b		6.94		6.94
⑨	$D = \frac{d_c}{L} \left(\frac{1}{1.0 - d_c/L} \right)$	⑤ $\left(\frac{1}{1.0 - \text{⑤}} \right)$		0.0465	0.1110	0.0465
⑩	$4 + G/2$	$4 + G/2$		7.47	13.38	7.47
⑪	$4 - G/2$	$4 - G/2$		0.527	-5.38	0.527
⑫	$D(4 + G/2)$	⑨ \times ⑩		0.348	1.488	0.348
⑬	$D(4 - G/2)$	⑨ \times ⑪		0.0245	-0.598	0.0245
⑭	$B = M_B/M_p$	1.0 or 0.0(lee end)		1.0	1.0	1.0
⑮	BR	⑥ \times ⑭		3.49	9.38	3.49
⑯	$G - BR$	$G - \text{⑮}$		3.45	9.38	3.45
BOTH ENDS RIGID						
⑰	M_1/M_{pm}	⑫ + ⑮		3.838	10.868	3.838
⑱	M_2/M_{pm}	⑯ - ⑬		3.426	9.978	3.426
LEE REAL HINGE (B=0)						
⑲	M_1/M_{pm}	⑫				
⑳	M_2/M_{pm}	$G - \text{⑬}$				
WINDWARD REAL HINGE (A=0)						
㉑	M_1/M_{pm}	⑥ + ⑫				
㉒	M_2/M_{pm}	- ⑬				
WIND FROM LEFT						
㉓	M_1 (right end)	① $\times M_1/M_{pm}$	kip-feet	369	312	369
㉔	M_2 (left end)	① $\times M_2/M_{pm}$	kip-feet	329	286	329
WIND FROM RIGHT						
㉕	M_1 (left end)	-① $\times M_1/M_{pm}$	kip-feet	-369	-312	-369
㉖	M_2 (right end)	-① $\times M_2/M_{pm}$	kip-feet	-329	-286	-329

^a With one real hinge use R/2 instead of ⑥.^b With lee real hinge use R/2 instead of ⑥.

TABLE A4. - HINGE FORMATION SEQUENCE,
SUBASSEMBLAGES A AND B

Line	Function	Operation	Units	Column A		Column B			
				Girder AB		Girder AB		Girder BC	
				Left	Right	Left	Right	Left	Right
①	Limiting M		kip-feet	329	369	329	369	286	312
②	Initial M		kip-feet	-137	144	-137	144	-59	59
③	∂M Possible	① - ②	kip-feet	466	225	466	225	345	253
④	Relative k_r			1	1	1	1	1	1
⑤	^a Relative G_r	④ × ($\frac{I}{L_g}$)	$\frac{\text{inches}^4}{\text{foot}}$	36.1	36.1	36.1	36.1	72.5	72.5
⑥	Joint Stiffness	$\Sigma G_r = \Sigma ⑤$	$\frac{\text{inches}^4}{\text{foot}}$	36.1				108.6	
⑦	Relative $\partial\theta_r$	③ / ⑤	$\frac{\text{kip-feet}^2}{\text{inches}^4}$	12.92	6.24	12.92	6.24	4.76	3.50
⑧	Actual $\partial\theta_r$	Min. ⑦	$\frac{\text{kip-feet}^2}{\text{inches}^4}$	6.24				3.50	
⑨	Actual ∂M	⑤ × ⑧	kip-feet	225	225	126	126	253	253
⑩	M, End of Step	② + ⑨	kip-feet	88	369	-11	270	194	312
⑪	ΣM at Joint	From ⑩	kip-feet	88				464	
⑫	Column M	⑪ / 2	kip-feet	44				232	
⑬	Hinge Formed	⑩ or ⑫		Hinge B	X			Hinge C	X
⑭	∂ M Possible	① - ⑩	kip-feet	241	0	340	99	92	0
⑮	Relative k_r			1/2	0	1	1	1/2	0
⑯	^a Relative G_r	⑮ × $\frac{I}{L_g}$	$\frac{\text{inches}^4}{\text{foot}}$	18.05	0	36.1	36.1	36.25	0
⑰	Joint Stiffness	$\Sigma G_r = \Sigma ⑯$	$\frac{\text{inches}^4}{\text{foot}}$	18.05			72.35		
⑱	Relative $\partial\theta_r$	⑭ / ⑯	$\frac{\text{kip-feet}^2}{\text{inches}^4}$	13.33	0	9.40	2.74	2.54	2.38
⑲	Actual $\partial\theta_r$	Min. ⑱	$\frac{\text{kip-feet}^2}{\text{inches}^4}$	13.33				2.38	
⑳	Actual ∂M	⑯ × ⑲	kip-feet	241	0	85.5	85.6	86.2	
㉑	M, End of Step	⑩ + ⑳	kip-feet	329	369	74.5	355.6	280.2	
㉒	ΣM at Joint	From ㉑	kip-feet	329				635.8	
㉓	Column M	㉒ / 2	kip-feet	164.5				317.9	
㉔	Hinge Formed	㉑ or ㉓		X	Hinge A	Column Hinge	X		

^a Use $\frac{I}{L_g} (1-d_c/L)$ when using clear span statics.

TABLE A5. - HINGE FORMATION SEQUENCE,
SUBASSEMBLAGES C AND D

Line	Function	Operation	Units	Column C				Column D ^a	
				Girder BC		Girder CD		Girder CD	
				Left	Right	Left	Right	Left	Right
①	Limiting M		kip-feet	286	312	329	369	329	369
②	Initial M		kip-feet	-59	59	-144	137	-144	137
③	∂M Possible	① - ②	kip-feet	345	253	473	232	473	232
④	Relative k_r			1	1	1	1	1	1
⑤	^a Relative G_r	④ × ($\frac{I}{L_g}$)	$\frac{\text{inches}^4}{\text{feet}}$	72.5	72.5	36.1	36.1	36.1	36.1
⑥	Joint Stiffness	$\Sigma G_r = \times ⑤$	$\frac{\text{inches}^4}{\text{feet}}$			108.6			36.1
⑦	Relative $\partial\theta_r$	③ / ⑤	$\frac{\text{kip-feet}^2}{\text{inches}^4}$	4.76	3.50	13.1	6.44	13.1	6.44
⑧	Actual $\partial\theta_r$	Min. ⑦	$\frac{\text{kip-feet}^2}{\text{inches}^4}$			3.50			6.44
⑨	Actual ∂M	⑤ × ⑧	kip-feet	253	253	126	126	232	232
⑩	M, End of Step	② + ⑨	kip-feet	194	312	-18	263	88	369
⑪	ΣM at Joint	From ⑩	kip-feet			294			369
⑫	Column M	⑪ / 2	kip-feet			147			184.5
⑬	Hinge Formed	⑩ or ⑫		Hinge C	X			Hinge D	X
⑭	∂ M Possible	① - ⑩	kip-feet		0 ⁸³	347	106		0
⑮	Relative k_r				0	1	1		0
⑯	^a Relative G_r	⑮ × $\frac{I}{L_g}$	$\frac{\text{inches}^4}{\text{feet}}$		0	36.1	36.1		
⑰	Joint Stiffness	$\Sigma G_r = \times ⑯$	$\frac{\text{inches}^4}{\text{feet}}$			36.1			
⑱	Relative $\partial\theta_r$	⑭ / ⑯	$\frac{\text{kip-feet}^2}{\text{inches}^4}$			2.31	9.61		
⑲	Actual $\partial\theta_r$	Min. ⑱	$\frac{\text{kip-feet}^2}{\text{inches}^4}$			2.31			
⑳	Actual ∂M	⑯ × ⑲	kip-feet			83.2	83.2		
㉑	M, End of Step	⑩ + ⑳	kip-feet		312	65.2	346.2		
㉒	ΣM at Joint	From ㉑	kip-feet			377.2			
㉓	Column M	㉒ / 2	kip-feet			188.6			
㉔	Hinge Formed	㉑ or ㉓		Column hinge	X				

^a Use $\frac{I}{L_g}$ (1-d_c/L) when using clear span statics.

TABLE A6. - SUBASSEMBLAGE SHEAR VERSUS DRIFT

Line	Function	Operation	Units	Subassemblages				Data
				A	B	C	D	
				626	626	858	812	P
			$\frac{\text{kip-feet}}{\text{inches}^4}$	3.02×10^{-6}	3.02×10^{-6}	3.17×10^{-6}	3.12×10^{-6}	$\frac{\gamma'}{2M_{pc}}$
①	Relative $\partial \theta_R$			6.24	3.50	3.50	6.44	
②	$\partial \theta_R \times \Sigma G_R$	$\frac{② \times \gamma'}{2.0 M_{pc}}$	kip-feet	225	380	380	232	
③	Part 1, $\partial \Delta/h$	$(24.0/E) \times ①$	radians	0.000680	0.001150	0.001207	0.000724	
④	Part 2, $\partial \Delta/h$		radians	0.00516	0.00290	0.00290	0.00532	
⑤	$\partial \Delta/h$	③ + ④	radians	0.00584	0.00405	0.00411	0.00604	
⑥	Part 1, ∂Q	② / h	kips	23.3	39.4	39.4	24.0	
⑦	Part 2, ∂Q	⑤ $\times P$	kips	3.7	2.5	3.5	4.9	
⑧	∂Q	⑥ - ⑦	kips	19.6	36.9	35.9	19.1	
⑨	Q at start		kips	-14.2	8.9	-8.9	14.2	DATA 2
⑩	Q at end	⑧ + ⑨	kips	5.4	45.8	27.0	33.3	DATA 2
⑪	Δ/h at start		radians	0	0	0	0	DATA 1
⑫	Δ/h at end	⑤ + ⑪	radians	0.00584	0.00405	0.00411	0.00604	DATA 1
⑬	Sequence of Δ/h	⑫, ⑭ or ⑮		3	1	2	4	DATA 4
⑭	Graph Slope	⑧ / ⑤	kips/rad	3360	9120	8740	3160	DATA 3
⑮	Relative $\partial \theta_R$		$\frac{\text{kip-feet}}{\text{inches}^4}$	13.33	2.38	2.31		
⑯	$\partial \theta_R \times \Sigma G_R$	$\frac{⑯ \times \gamma'}{2.0 M_{pc}}$	kip-feet	241	172	83		
⑰	Part 1, $\partial \Delta/h$	$(24.0/E) \times ⑮$	radians	0.00073	0.00052	0.00026		
⑱	Part 2, $\partial \Delta/h$		radians	0.01103	0.00197	0.00191		
⑲	$\partial \Delta/h$	⑰ + ⑱	radians	0.01176	0.00249	0.00217	0.01896	
⑳	Part 1, ∂Q	⑯ / h	kips	24.9	17.8	8.6		
㉑	Part 2, ∂Q	⑲ $\times P$	kips	7.4	1.6	1.9	15.4	
㉒	∂Q	⑲ - ㉑	kips	17.5	16.2	6.7	-15.4	
㉓	Q at end	⑩ + ㉒	kips	22.9	62.0	33.7	17.9	DATA 2
㉔	Δ/h at end	⑫ + ⑲	radians	0.01760	0.00654	0.00628	0.025	DATA 1
㉕	Sequence of Δ/h	⑫, ⑭ or ⑮		7	6	5	8	DATA 4
㉖	Graph Slope	㉒ / ⑲	kips/rad	1490	6500	3080	-812	DATA 3
㉗	Relative $\partial \theta_R$		$\frac{\text{kip-feet}}{\text{inches}^4}$					
㉘	$\partial \theta_R \times \Sigma G_R$	$\frac{㉘ \times \gamma'}{2.0 M_{pc}}$	kip-feet					
㉙	Part 1, $\partial \Delta/h$	$(24.0/E) \times ㉗$	radians					
㉚	Part 2, $\partial \Delta/h$		radians					
㉛	$\partial \Delta/h$	㉙ + ㉚	radians	0.00740	0.01846	0.01872		
㉜	Part 1, ∂Q	㉘ / h	kips					
㉝	Part 2, ∂Q	㉛ $\times P$	kips	4.6	11.6	16.1		
㉞	∂Q	㉛ - ㉝	kips	-4.6	-11.6	-16.1		
㉟	Q at end	㉛ + ㉞	kips	18.3	50.4	17.6		DATA 2
㊱	Δ/h at end	㉛ + ㉚	radians	0.025	0.025	0.025		DATA 1
㊲	Sequence of Δ/h	⑫, ⑭ or ⑮		8	8	8		DATA 4
㊳	Graph Slope	㉞ / ㉛	kips/rad	-626	-626	-858		DATA 3

TABLE A7. - STORY Q VERSUS Δ/h

Line	Function	Operation	Units	Subassemblages				Total Story	Data 4
				A	B	C	D		
①	Δ/h at start	DATA 1	radians					0.0	1
②	Q at start	DATA 2	kips					0.0	
③	Graph Slope	DATA 3	kips/rad	3360	9120	8740	3160	24380	
④	Δ/h at end	DATA 1	radians					0.00405	
⑤	Δ/h increment	④ - ①	radians					0.00405	
⑥	∂Q	③ x ⑤	kips					98.9	
⑦	Q at end	② + ⑥	kips					98.9	
⑧	Subassemblage After Slope								
⑨	Graph Slope	DATA 3	kips/rad	3360	6500	8740	3160	21760	2
⑩	Δ/h at end	DATA 1	radians					0.00411	
⑪	Δ/h increment	⑩ - ④	radians					0.00006	
⑫	∂Q	⑨ x ⑪	kips					1.3	
⑬	Q at end	⑦ + ⑫	kips					100.2	
⑭	Subassemblage After Slope								
⑮	Graph Slope	DATA 3	kips/rad	3360	6500	3080	3160	16100	3
⑯	Δ/h at end	DATA 1	radians					0.00584	
⑰	Δ/h increment	⑯ - ⑩	radians					0.00173	
⑱	∂Q	⑮ x ⑰	kips					27.8	
⑲	Q at end	⑬ + ⑱	kips					128.0	
⑳	Subassemblage After Slope								
㉑	Graph Slope	DATA 3	kips/rad	1490	6500	3080	3160	14230	4
㉒	Δ/h at end	DATA 1	radians					0.00604	
㉓	Δ/h increment	㉒ - ⑯	radians					0.00020	
㉔	∂Q	㉑ x ㉓	kips					2.8	
㉕	Q at end	⑲ + ㉔	kips					130.8	
㉖	Subassemblage After Slope								

TABLE A7 (CONTINUED). - STORY Q VERSUS Δ/h .

Line	Function	Operation	Units	Subassemblages				Total Story	Data
				A	B	C	D		
(27)	Graph Slope	DATA 3	kips/rad	1490	6500	3080	-815	10258	5
(28)	Δ/h at end	DATA 1	radians					0.00628	
(29)	Δ/h increment	(28) - (22)	radians					0.00024	
(30)	∂Q	(27) x (29)	kips					2.5	
(31)	Q at end	(25) + (30)	kips					133.3	
(32)	Subassemblage After Slope					X			
(33)	Graph Slope	DATA 3	kips/rad	1490	6500	-858	-812	6320	6
(34)	Δ/h at end	DATA 1	radians					0.00654	
(35)	Δ/h increment	(34) - (28)	radians					0.00026	
(36)	∂Q	(33) x (35)	kips					1.6	
(37)	Q at end	(31) + (36)	kips					134.9	
(38)	Subassemblage After Slope				X				
(39)	Graph Slope	DATA 3	kips/rad	1490	-626	-858	-812	-806	7
(40)	Δ/h at end	DATA 1	radians					0.01760	
(41)	Δ/h increment	(40) - (34)	radians					0.01106	
(42)	∂Q	(39) x (41)	kips					-8.9	
(43)	Q at end	(37) + (42)	kips					126.0	
(44)	Subassemblage After Slope			X					
(45)	Graph Slope	DATA 3	kips/rad	-626	-626	-858	-812	-2922	8
(46)	Δ/h at end	DATA 1	radians					0.02500	
(47)	Δ/h increment	(46) - (40)	radians					0.00740	
(48)	∂Q	(45) x (47)	kips					-21.6	
(49)	Q at end	(43) + (48)	kips					104.4	
(50)	Subassemblage After Slope			END					

APPENDIX II. - REFERENCES

1. Daniels, J.H.
COMBINED LOAD ANALYSIS OF UNBRACED FRAMES,
Ph.D. Dissertation, Lehigh University, 1967,
University Microfilms, Inc., Ann Arbor, Michigan.
2. Daniels, J.H.
A PLASTIC METHOD FOR UNBRACED FRAME DESIGN,
Engineering Journal, AISC, Vol. 3, No. 4, October 1966,
p. 141-149.
3. Driscoll, G. C., Jr., et al.
PLASTIC DESIGN OF MULTI-STORY FRAMES --
LECTURE NOTES, Fritz Engineering Laboratory Report
273.20, Lehigh University, 1965.
4. Parikh, B. P., Daniels, J. H., and Lu, L. W.
PLASTIC DESIGN OF MULTI-STORY FRAMES -- DESIGN AIDS,
Fritz Engineering Laboratory Report 273.24, Lehigh University,
1965.
5. Daniels, J. H. and Lu, L. W.
THE SUBASSEMBLAGE METHOD OF DESIGNING UNBRACED
MULTI-STORY FRAMES, Fritz Engineering Laboratory
Report No. 273.37, Lehigh University, March 1966.
6. Daniels, J. H. and Lu, L. W.
DESIGN CHARTS FOR THE SUBASSEMBLAGE METHOD OF
DESIGNING UNBRACED MULTI-STORY FRAMES, Fritz Engineering
Laboratory Report No. 273.54, Lehigh University,
November 1966.
7. Driscoll, G. C. and Armacost, J. O.
THE COMPUTER ANALYSIS OF UNBRACED MULTI-STORY FRAMES,
Fritz Engineering Laboratory Report No. 345.5,
Lehigh University, 1968, DDC Document AD670 742,
Clearing house.

APPENDIX III. - NOTATION

The following symbols are used in this paper:

A = parameter for moment at windward end divided by plastic hinge moment;

B = parameter for moment at lee end divided by plastic hinge moment;

C = parameter with column depth and beam spacing;

DF = distribution factor;

d_c = depth of column;

E = modulus of elasticity;

FEM = fixed end moment;

F_y = yield point stress;

G = sum of girder moments parameter;

G_R = relative girder stiffness;

H = horizontal shear on a story;

h = story height;

I = moment of inertia;

k_R = relative stiffness coefficient;

L = length of girder;

L_g = clear span length of girder;

M = moment;

M_A = moment at windward end of clear span;

M_B = moment at lee end of clear span;

M_{BL} = girder moment left of joint;

M_{BR} = girder moment right of joint;

M_C^o = original moment at top of column;

M_p = plastic hinge moment;

M_{pc} = plastic hinge moment with axial compression

M_{pm} = minimum plastic moment parameter;
 M_r = restraining moment;
 M_u = moment at upper end of column;
 M_1 = girder moment at lee column centerline;
 M_2 = girder moment at windward column centerline;
 P = column thrust;
 P_y = column yield thrust;
 Q = column or subassembly shear;
 Q_0 = initial value of shear;
 R = ratio of plastic moment to minimum plastic moment;
 r_x = radius of gyration about strong axis;
 w = uniform load;
 Z = plastic section modulus;
 α = portion of story height from column top to inflection point;
 β = portion of girder moment sum to be distributed to column top;
 γ = angle between column chord and column centerline tangent;
 γ' = limiting column chord angle;
 Δ = horizontal drift of a story;
 θ = rotation of a joint;